Å. In both cases, the longer Fe–N_p bond is the one approximately perpendicular to the parallel imidazole planes. In high-spin iron(III) both of the relevant d_π orbitals are half filled. However, the porphyrin does not compete with imidazole for L to M π-donation with the orbital parallel to the imidazole planes. Hence, the porphyrin to Fe bonding is expected to be stronger in this direction and the Fe–N_p bond parallel to the imidazole planes is the shorter bond.[21,22]

The axial bond distances in the two independent ions of [Fe(TPP)(HIm)$_2$]Cl·CHCl$_3$·H$_2$O are also different. The length in ion A is 1.977 (3) Å, while the value in ion B is 1.964 (3) Å. The original report by Hoard et al.[1] provides the basis for expecting and understanding this effect. As pointed out by Hoard et al., the imidazole ligand with the smaller value of ϕ has more significant nonbonded interactions between axial ligand and the core and hence a longer axial bond distance is expected. These expectations are met in [Fe(TPP)(HIm)$_2$]Cl·CHCl$_3$·H$_2$O, and as noted, ion A has the smaller value of ϕ. The range of values for the axial bonds, previously observed, is from 1.957 to 1.991 Å.

Figure 4 also presents the displacements of the atoms from the mean plane of the respective 24-atom core. In neither ion are the deviations from planarity remarkable. The deviation from planarity of all units expected to be planar (imidazole rings, peripheral phenyls, and pyrrole rings) is less than 0.01 Å. The imidazole plane in ion A forms a dihedral angle of 86.4° with the porphyrin core; the corresponding value in ion B is 87.0°. The dihedral angles between the peripheral phenyl rings in ion A are 68.9 and 81.9°, and for ion B the values are 72.6 and 85.7°. There are no unusual intermolecular contacts.

Summary. The axial imidazole ligand orientation leads to effects in the lengths of the equatorial bonds in addition to the better-known correlation with the length of the axial bonds. This equatorial effect appears to result from competition between the porphyrin and imidazole to π-donate to the iron(III). The imidazole orientation effect also appears to lead to experimentally definable variations in the EPR spectrum and would allow, in principle, a definition of geometrical aspects of bis(imidazole) hemes and hemoproteins from the spectrum.

Note Added in Proof. Strouse et al.[23] have found that the low-spin complex bis(*cis*-methylurocanate)(*meso*-tetraphenylporphinato)iron(III) shows some similar effects. They find two different orientations of the parallel substituted imidazole ligands with ϕ = 16 and 29° and two overlapping "normal" EPR spectra. They have been able to fit the entire set of four observed ligand orientations and EPR spectra to a crystal field model. This study confirms our tentative assignments of EPR spectra with orientation angle. In addition, they observe a similar rhombicity of the equatorial Fe–N bond distances for the ϕ = 16° complex.

Acknowledgment. We thank the National Institutes of Health for support under Grant HL-15627 and Prof. F. A. Walker for useful discussions.

Registry No. [Fe(TPP)(HIm)$_2$]Cl, 25442-52-8.

Supplementary Material Available: Table IS, anisotropic temperature factors, and Table IIS, fixed hydrogen atom coordinates for [Fe(TPP)(HIm)$_2$]Cl·CHCl$_3$·H$_2$O (3 pages); listings of the observed and calculated structure amplitudes (×10) (19 pages). Ordering information is given on any current masthead page.

(20) Levan, K. R.; Strouse, C. E. *Abstract of Papers*: Americal Crystallolgraphic Association Summer Meeting, Snowmass, CO, Aug 1-5, 1983; Abstract H1. Levan, K. R. Ph.D. Thesis, UCLA, 1984.

(21) Note that the direction of the "back-bonding" mechanism in iron(III) porphyrinates is different for five- and six-coordinate high-spin iron(III) species. Six-coordinate derivatives have the same direction as low-spin iron(III) complexes.[22] Cf, Goff, H. M.; Shimomura, E. T.; Phillippi, M. A. *Inorg. Chem.* **1983**, *22*, 66-71.

(22) La Mar, G. N.; Walker, F. A. In *The Porphyrins*; Dolphin, D., Ed.; Academic Press: New York, 1979; Vol. IV, pp 61-157.

(23) Quinn, R.; Valentine, J. S.; Byrn, M. P.; Strouse, C. E. *J. Am. Chem. Soc.*, in press.

Unusual Orientation of Axial Ligands in Metalloporphyrins. Molecular Structure of Low-Spin Bis(2-methylimidazole)(*meso*-tetraphenylporphinato)iron(III) Perchlorate

W. Robert Scheidt,*[1] John F. Kirner, J. L. Hoard,*[2] and Christopher A. Reed*[3]

Contribution from the Departments of Chemistry, University of Notre Dame, Notre Dame, Indiana 46556, Cornell University, Ithaca, New York 14850, and the University of Southern California, Los Angeles, California 90089-1062. *Received October 15, 1986*

Abstract: The preparation and characterization of the low-spin complex [Fe(TPP)(2-MeHIm)$_2$]ClO$_4$ is described. The detailed temperature-dependent magnetic susceptibility of two different solvates and the crystal structure determination of the tetrahydrofuran solvate are reported. Solid samples of both solvates of [Fe(TPP)(2-MeHIm)$_2$]ClO$_4$ have an unusual low-spin EPR spectrum, the so-called "strong g_{max}" signal. This strong g_{max} signal is correlated with a mutually perpendicular alignment of the two axial 2-methylimidazole ligands. This arrangement solves certain stereochemical problems associated with the formation of the low-spin iron(III) complex with the sterically hindered axial ligands. In addition, the short axial bond required for the low-spin state is achieved by a tipping of the axial ligands and a substantial S_4 ruffling of the porphinato core. A detailed analysis and comparison of this structure and that of a related high-spin complex with the same axial ligands ([Fe(OEP)(2-MeHIm)$_2$]ClO$_4$) is given. This analysis shows the subtlety of the steric interactions of the methyl protons with porphinato core atoms. The axial Fe–N bond distance average is 2.012 Å, and the equatorial bond distance average is 1.970 Å. Crystal data for [Fe(TPP)(2-MeHIm)$_2$]ClO$_4$·THF·H$_2$O: monoclinic, a = 26.943 (3) Å, b = 16.927 (2) Å, c = 23.358 (3) Å, and β = 104.76 (1)°, Z = 8, space group $C2/c$, 6648 observed data.

The structural characterization of [Fe(TPP)(2-MeHIm)$_2$]ClO$_4$[4] was undertaken as part of our program to understand the control of structure, spin state, and other physical properties in (porphinato)iron species. As is well-known, (porphinato)iron(II) and

0002-7863/87/1509-1963$01.50/0

-(III) species readily add two nitrogen donor ligands. For the binding of such axial ligands,[5] K_2 is greater than K_1 and the resulting bis complexes are low-spin species. This binding constant order, in which K_2 is typically more than one order of magnitude larger than K_1, leads to difficulties in synthesizing five-coordinate derivatives and mixed-ligand six-coordinate derivatives. Recently, five-coordinate species with neutral nitrogen donors have been prepared by control of stoichiometry in octaethylporphyrin complexes where porphyrin π–π dimer formation gives added stability to five-coordinate species, at least in the solid state.[6,7] Blocking one face of the metalloporphyrin complex can also be used as a means of preparing five-coordinate species,[8] but crystallographic characterization has yet to be reported. However, the oldest and commonest approach to such syntheses, first employed by Collman and Reed,[9] is the use of a sterically hindered axial ligand such as 2-methylimidazole. In such cases, it was expected that the sterically hindered imidazole would reduce the magnitude of K_2 without significantly changing the first binding constant because steric constraints in bis-ligated species are largely relieved by movement of the iron and ligand away from the porphyrin in a mono-ligated species.

For ferrous porphyrinates this expectation was realized in the isolation[9] of the monoimidazole complex [Fe(TPP)(2-MeHIm)]·C_2H_5OH, although in solution a second 2-methylimidazole ligand is reported to bind at low temperature.[10] For ferric porphyrinates, however, this strategy has not been found to be as appropriate. Six-coordination occurs, but curiously both high-spin and low-spin bis(2-methylimidazole) ferric porphyrinates are now known. The high-spin complex, [Fe(OEP)(2-MeHIm)$_2$]ClO_4, was reported in a recent paper from our laboratories.[11] Low-spin [Fe(TPP)(2-MeHIm)$_2$]ClO_4, although known for some time,[12] has not been fully described.

The high-spin state is consistent with the sterically bulky nature of the axial ligands because the long axial bonds appropriate[13] to this state are a natural consequence of limited approach of the methyl groups toward the porphyrin core. On the other hand, a low-spin complex, with its concomitant short axial bonds, is expected to lead to substantial steric interaction between the methyl groups and the core. Thus, the observation that two sterically bulky 2-methylimidazole ligands coordinate to (tetraphenylporphinato)iron(III) to yield a six-coordinate low-spin species is unexpected. We have determined the molecular structure of the tetrahydrofuran solvate of low-spin [Fe(TPP)(2-MeHIm)$_2$]ClO_4 to determine the stereochemical solution to the apparent steric problems. Briefly, we find that the steric difficulties between the axial ligands and equatorial porphyrin are ameliorated, by a significant S_4 ruffling of the porphinato core, by specific, favorable orientations of the axial ligands with respect to the core and by a perpendicular alignment of the two axial ligand planes. These findings are analyzed in detail by comparing them to the steric interactions in the related high-spin species. Despite significant structural differences in the high- and low-spin compounds, the steric interactions in the two complexes remain relatively similar. This serves to emphasize the subtle nature of steric hindrance in 2-methylimidazole systems.

The perpendicular alignment of the two axial ligand planes is of particular interest in correlating the effects of axial ligand orientation on the physical properties of heme derivatives. In particular, this alignment of the axial ligands is discussed in terms of the strong g_{max} EPR signal observed for a limited number of low-spin ferric species.

Experimental Section

[Fe(TPP)($OClO_3$)]·*m*-xylene[14] (100 mg) and 2-methylimidazole (40 mg) were dissolved in tetrahydrofuran (15 mL). After letting the mixture stand overnight crystals suitable for X-ray analysis were deposited. Anal. Calcd for $FeClO_5N_8C_{56}H_{48}$: C, 66.95; H, 4.8; N, 11.5. Found: C, 66.45; H, 5.05; N, 11.0. A chloroform solvate, rather than a THF solvate, can be prepared by substitution of chloroform as solvent. The magnetic susceptibility of both solvates was determined in the solid state over the temperature range 6–300 K on a SHE SQUID susceptometer.

Single crystals of the THF solvate of [Fe(TPP)(2-MeHIm)$_2$]ClO_4 were subjected to a preliminary photographic examination. This showed an eight-molecule monoclinic unit cell; the systematic absences suggest the space groups *Cc* or *C*2/*c*. The centrosymmetric choice was suggested by the *E* statistics and confirmed by all subsequent developments during structure solution and refinement. A crystal with approximate dimensions of 0.09 × 0.27 × 0.75 mm was mounted in a glass capillary and used for the measurement of precise cell constants and intensity data collection. These data were measured with Ni-filtered Cu Kα (λ 1.54178 Å) radiation on a Picker FACS-I automated diffractometer. Least-squares refinement of 49 reflections, each measured at $\pm 2\theta$, led to the lattice constants a = 26.943 (3) Å, b = 16.927 (2) Å, c = 23.358 (3) Å, and β = 104.76 (1)°. The experimental density was 1.32 g/cm^3; the calculated density for [Fe(TPP)(2-MeHIm)$_2$]ClO_4·THF·H_2O is 1.318 g/cm^3.

Diffracted intensities were measured with θ–2θ scans with a base width of 1.8° and a fixed scan rate of 1 deg/min. Background counts were of 40 s duration at the extremes of each scan. Three standard reflections, measured after each 50 reflections, showed a small (<3%) decrease with time; no correction was made. An analytical absorption correction was applied to the data with use of a linear absorption coefficient of 3.27 mm^{-1} for Cu Kα radiation. A total of 7652 reflections with $(\sin\theta)/\lambda < 0.562$ Å^{-1} were measured. Intensity data were reduced as described previously[15] and 6648 data with $F_o > 1.58\sigma(F_o)$ were retained as observed and used in all subsequent calculations.

The structure was solved by the standard heavy-atom method and refined by full-matrix least-squares techniques.[16] During refinement, an extinction correction was made by using the function $f(x) = 1/(1 + 2x)^{1/2}$.[17] The THF molecule was refined as a rigid body owing to disorder in the crystal. A difference Fourier calculated after isotropic refinement suggested the presence of a water of solvation and also revealed electron density appropriate for all porphinato and ring imidazole hydrogen atom positions. Subsequent calculations suggested positions for five of the six methyl hydrogen atoms of the two imidazole ligands (vide infra). All hydrogen atom positions were idealized (C–H = 0.95 Å, B(H) = B(C) = 1.0 Å^2) and included as fixed contributors in subsequent refinement cycles. Refinement was then carried to convergence with anisotropic thermal parameters for all heavy atoms save those of the THF and water solvates. At convergence, discrepancy indices R_1 = 0.089 and R_2 = 0.096.[18] Final atomic coordinates are listed in Table I, and

(1) University of Notre Dame.
(2) Cornell University.
(3) University of Southern California.
(4) Abbreviations used: TPP, OEP, and TpivPP, dianions of *meso*-tetraphenylporphyrin, octaethylporphyrin, and picket fence porphyrin; 2-MeHIm, 2-methylimidazole, HIm, imidazole; 1-MeIm, 1-methylimidazole; 1,2-DiMeIm, 1,2-dimethylimidazole; BzHIm, benzimidazole; THF, tetrahydrofuran; N_p, porphinato nitrogen.
(5) Walker, F. A.; Lo, M.-W.; Ree, M. T. *J. Am. Chem. Soc.* **1976**, *98*, 5552–5560. Walker, F. A.; Barry, J. A.; Balke, V. L.; McDermott, G. A.; Wu, M. Z.; Linde, P. F. *Adv. Chem. Ser.* **1982**, *201*, 377–416.
(6) Scheidt, W. R.; Geiger, D. K.; Lee, Y. J.; Reed, C. A.; Lang, G. *J. Am. Chem. Soc.* **1985**, *107*, 5693–5699.
(7) Scheidt, W. R.; Geiger, D. K.; Lee, J. Y.; Reed, C. A.; Lang, G. *Inorg. Chem.*, submitted.
(8) Hashimoto, T.; Dyer, R. L.; Crossley, M. J.; Baldwin, J. E.; Basolo, F. *J. Am. Chem. Soc.* **1982**, *104*, 2101–2109. Momentau, M.; Loock, V.; Tetreau, C.; Lavalette, D.; Croisy, A.; Schaeffer, C.; Huel, C.; Lhoste, J.-M. *J. Chem. Soc., Perkin Trans. 2*, in press. Collman, J. P.; Brauman, J. I.; Iverson, B. L.; Sessler, J. L.; Morris, R. M.; Gibson, Q. H. *J. Am. Chem. Soc.* **1983**, *105*, 3052–3064. Traylor, T. G.; Tsuchiya, S.; Campbell, D.; Mitchell, M.; Stynes, D.; Koga, N. *J. Am. Chem. Soc.* **1985**, *107*, 604–614.
(9) Collman, J. P.; Reed, C. A. *J. Am. Chem. Soc.* **1973**, *95*, 2048–2049.
(10) Wagner, G. C.; Kassner, R. J. *Biochim. Biophys. Acta* **1975**, *392*, 319–327.
(11) Geiger, D. K.; Lee, Y. J.; Scheidt, W. R. *J. Am. Chem. Soc.* **1984**, *106*, 6339–6343.
(12) Kirner, J. F.; Hoard, J. L.; Reed, C. A. *Abstract of Papers*; 175th National Meeting of the American Chemical Society, Anaheim, CA, March 13–17, 1978; American Chemical Society; Washington, DC, 1978; INOR 14.
(13) Scheidt, W. R.; Reed, C. A. *Chem. Rev.* **1981**, *81*, 543–555.
(14) Reed, C. A.; Mashiko, T.; Bentley, S. P.; Kastner, M. E.; Scheidt, W. R.; Spartalian, K.; Lang, G. *J. Am. Chem. Soc.* **1979**, *101*, 2948–2958.
(15) Scheidt, W. R.; Hoard, J. L. *J. Am. Chem. Soc.* **1973**, *95*, 8281–8288.
(16) Programs used in this study included local modifications of Zalkin's FORDAP, Busing and Levy's ORFFE and ORFLS, and Johnson's ORTEP2. Atomic form factors were from the following: Cromer, D. T.; Mann, J. B. *Acta Crystallogr., Sect. A* **1968**, *A24*, 321–323. Real and imaginary corrections for anomalous dispersion in the form factor of the iron and chlorine atoms were from the following: Cromer, D. T.; Liberman, D. J. *J. Chem. Phys.* **1970**, *53*, 1891–1898.
(17) Zachariasen, W. H. *Acta Crystallogr., Sect. A* **1968**, *A24*, 421–427.

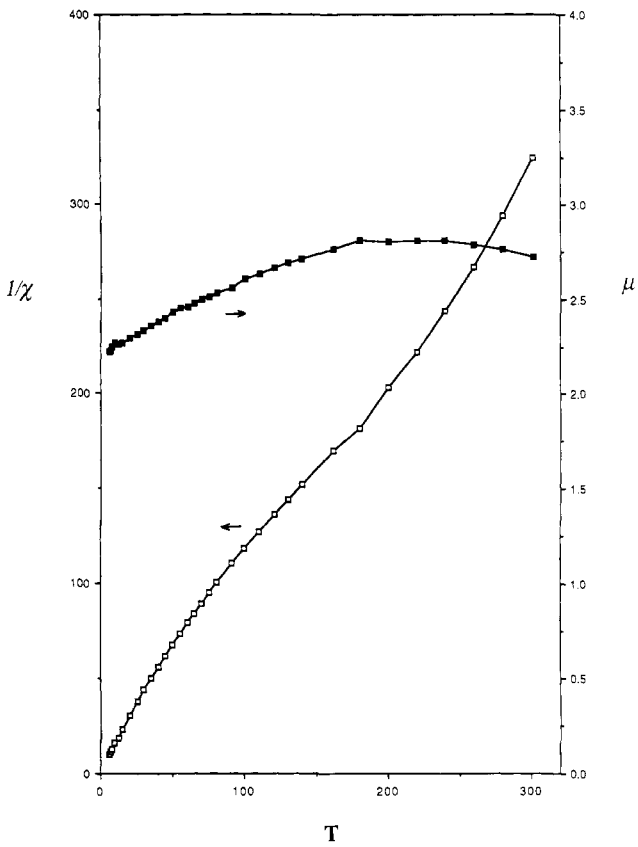

Figure 1. Plot of $1/\chi_m$ vs. T and μ_B vs. T for [Fe(TPP)(2-MeHIm)$_2$]-ClO$_4$·THF·H$_2$O.

final values of the thermal parameters and observed and calculated structure factors are available as supplementary material.

Results and Discussion

The assignment of a low-spin ferric state to [Fe(TPP)(2-MeHIm)$_2$]ClO$_4$ is consistent with all physical measurements. Solid state magnetic susceptibility data have been measured from 6 K to room temperature for the tetrahydrofuran and chloroform solvates. The data for the tetrahydrofuran solvate are shown in Figure 1. Data for the chloroform solvate are quite similar; complete magnetic data for both complexes are available as supplementary material. The room temperature moment of 2.7 μ_B is slightly higher than the normal value of 2.2–2.4 μ_B. The moments remain nearly constant to about 100 K and then fall off to 2.2 μ_B at 6 K. There is apparently almost no temperature-dependent data for low-spin (porphinato)iron(III) complexes available in the literature for comparison.[19] We had previously reported[11] solution susceptibility data in chloroform solution that showed some temperature dependence with μ = 2.73 μ_B at 309 K and decreasing to 2.55 μ_B at 248 K. We had interpreted that data as suggestive of a thermal spin equilibrium in solution. Given the closeness in energy between the high-spin and low-spin states this remains a reasonable hypothesis, but given the solid state moments reported above, this interpretation is less definitive than before.

An overall view of the structure of the [Fe(TPP)(2-MeHIm)$_2$]$^+$ ion is given in Figure 2. Figure 2 displays the atom labeling scheme used throughout this paper. Also shown in this figure are some bond distances in the coordination group. Individual values of bond distances and bond angles are displayed in Tables II and III, respectively. The average Fe-N$_p$ bond distance is 1.970 (4) Å. This value is slightly shorter than the 1.990-Å value typically observed[13,20,21] for other low-spin iron(III) porphyrinates. A few

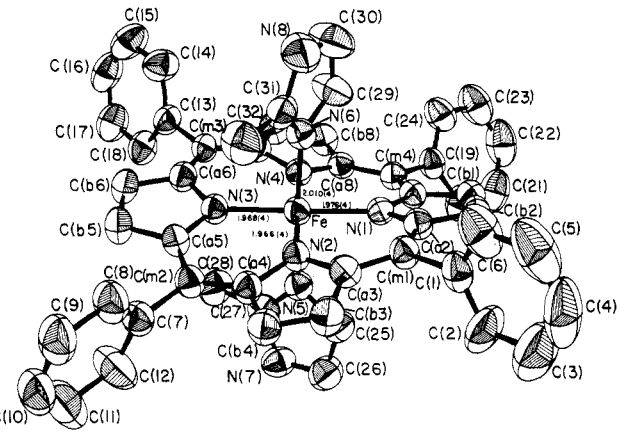

Figure 2. Computer-drawn model, in perspective, of the [Fe(TPP)(2-MeHIm)$_2$]$^+$ ion. Labels for all crystallographically unique atoms of the ion are displayed. 50% probability ellipsoids are shown for all atoms.

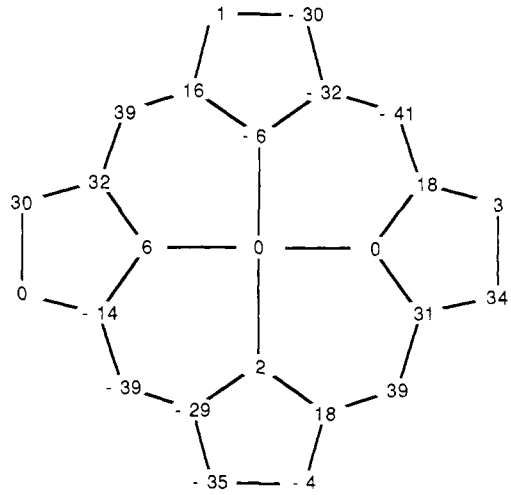

Figure 3. Formal diagram of the porphinato core displaying the values of the perpendicular displacements, in units of 0.01 Å, from the mean plane of the core. Positive values for displacements indicate a displacement toward the N(6) imidazole nitrogen atom. The diagram has the same relative orientation as that of Figure 2.

iron(III) species have comparable Fe–N$_p$ distances;[22] all have significantly S_4-ruffled cores. The stereochemical significance of this ruffling with respect to coordination of the bulky imidazole ligands will be discussed subsequently. Deviations of the atoms from the mean plane of the 24-atom core (in units of 0.01 Å) are shown in Figure 3; positive values of displacement of atoms are toward the N(6) imidazole nitrogen atom. Although not required in the crystal, the pattern of displacements is in agreement with exact S_4 symmetry. All individual imidazole, pyrrole, and phenyl rings are planar to within 0.01 Å. The values of the dihedral angles between the peripheral phenyl groups and the mean plane of the core are 61.6, 77.5, 75.2, and 89.5°. All but the first value are normal.[23]

(18) $R_1 = \sum||F_o| - |F_c||/\sum|F_o|$ and $R_2 = [\sum w(|F_o| - |F_c|)^2/\sum w(F_o)^2]^{1/2}$.
(19) Mitra, S. In *Iron Porphyrins*, Part II; Lever, A. B. P., Gray, H. B., Eds.; Addison-Wesley, Reading MA, 1983; pp 1–39.

(20) (a) Collins, D. M.; Countryman, R.; Hoard, J. L. *J. Am. Chem. Soc.* **1972**, *94*, 2066–2072. (b) Little, R. G.; Dymock, K. R.; Ibers, J. A. *J. Am. Chem. Soc.* **1975**, *97*, 4532–4539. (c) Quinn, R.; Strouse, C. E.; Valentine, J. S. *Inorg. Chem.* **1983**, *22*, 3934–3940. (d) Scheidt, W. R.; Osvath, S. R.; Lee, Y. J. *J. Am. Chem. Soc.*, preceding article in this issue.
(21) (a) Adams, K. M.; Rasmussen, P. G.; Scheidt, W. R.; Hatano, K. *Inorg. Chem.* **1979**, *18*, 1892–1899. (b) Scheidt, W. R.; Haller, K. J.; Hatano, K. *J. Am. Chem. Soc.* **1980**, *102*, 3017–3021. (c) Byrn, M. P.; Strouse, C. E. *J. Am. Chem. Soc.* **1981**, *103*, 2633–2635. (d) Scheidt, W. R.; Geiger, D. K.; Haller, K. J. *J. Am. Chem. Soc.* **1982**, *104*, 495–499. (e) Scheidt, W. R.; Lee, Y. L.; Geiger, D. K.; Taylor, K.; Hatano, K. *J. Am. Chem. Soc.* **1982**, *104*, 3367–3374. (f) Scheidt, W. R.; Lee, Y. J.; Hatano, K. *J. Am. Chem. Soc.* **1984**, *106*, 3191–3198.
(22) (a) Scheidt, W. R.; Lee, Y. J.; Luangdilok, W.; Haller, K. J.; Anzai, K.; Hatano, K. *Inorg. Chem.* **1983**, *22*, 1516–1522. (b) Doppelt, P. *Inorg. Chem.* **1984**, *23*, 4009–4011.

Table I. Fractional Atomic Coordinates in Crystalline $[Fe(TPP)(2\text{-MeHIm})_2]ClO_4 \cdot THF \cdot H_2O$

atom type	x	y	z
Fe	0.1642 (0)	0.0992 (0)	0.1473 (0)
Cl	0.0890 (1)	0.3465 (1)	0.3827 (1)
N(1)	0.1771 (2)	0.0582 (2)	0.2290 (2)
N(2)	0.2022 (2)	0.1964 (2)	0.1763 (2)
N(3)	0.1531 (2)	0.1382 (2)	0.0657 (2)
N(4)	0.1245 (2)	0.0030 (2)	0.1182 (2)
N(5)	0.1024 (2)	0.1577 (2)	0.1590 (2)
N(6)	0.2282 (2)	0.0421 (3)	0.1416 (2)
N(7)	0.0339 (2)	0.2317 (3)	0.1502 (2)
N(8)	0.3048 (2)	0.0047 (4)	0.1376 (2)
C(a1)	0.1561 (2)	−0.0083 (3)	0.2481 (2)
C(a2)	0.2133 (2)	0.0875 (3)	0.2779 (2)
C(a3)	0.2306 (2)	0.2120 (3)	0.2334 (2)
C(a4)	0.2007 (2)	0.2665 (3)	0.1457 (2)
C(a5)	0.1611 (2)	0.2132 (3)	0.0476 (2)
C(a6)	0.1354 (2)	0.0948 (3)	0.0139 (2)
C(a7)	0.1085 (2)	−0.0221 (3)	0.0602 (2)
C(a8)	0.1075 (2)	−0.0542 (3)	0.1515 (2)
C(b1)	0.1799 (2)	−0.0209 (3)	0.3103 (2)
C(b2)	0.2152 (2)	0.0369 (3)	0.3285 (2)
C(b3)	0.2469 (2)	0.2930 (3)	0.2382 (2)
C(b4)	0.2278 (2)	0.3272 (3)	0.1845 (2)
C(b5)	0.1485 (2)	0.2164 (4)	−0.0158 (2)
C(b6)	0.1335 (2)	0.1442 (4)	−0.0362 (2)
C(b7)	0.0802 (2)	−0.0944 (3)	0.0569 (2)
C(b8)	0.0791 (2)	−0.1131 (3)	0.1128 (2)
C(m1)	0.2384 (2)	0.1591 (3)	0.2809 (2)
C(m2)	0.1810 (2)	0.2759 (3)	0.0857 (2)
C(m3)	0.1151 (2)	0.0186 (3)	0.0113 (2)
C(m4)	0.1212 (2)	−0.0589 (3)	0.2128 (2)
C(1)	0.2721 (2)	0.1848 (3)	0.3401 (2)
C(2)	0.2508 (3)	0.2271 (5)	0.3774 (3)
C(3)	0.2798 (5)	0.2513 (6)	0.4308 (4)
C(4)	0.3295 (5)	0.2311 (6)	0.4472 (3)
C(5)	0.3527 (3)	0.1888 (5)	0.4117 (4)
C(6)	0.3226 (3)	0.1650 (4)	0.3565 (3)
C(7)	0.1853 (2)	0.3551 (3)	0.0591 (2)
C(8)	0.2311 (3)	0.3796 (4)	0.0498 (3)
C(9)	0.2352 (3)	0.4543 (4)	0.0248 (3)
C(10)	0.1937 (4)	0.5024 (4)	0.0096 (3)
C(11)	0.1474 (4)	0.4778 (5)	0.0167 (4)
C(12)	0.1432 (3)	0.4032 (4)	0.0417 (4)
C(13)	0.0951 (2)	−0.0194 (3)	−0.0482 (2)
C(14)	0.1237 (3)	−0.0755 (4)	−0.0685 (3)
C(15)	0.1035 (3)	−0.1131 (4)	−0.1231 (3)
C(16)	0.0552 (3)	−0.0935 (4)	−0.1559 (3)
C(17)	0.0272 (3)	−0.0382 (4)	−0.1363 (3)
C(18)	0.0470 (2)	−0.0006 (4)	−0.0818 (2)
C(19)	0.1019 (2)	−0.1261 (3)	0.2424 (2)
C(20)	0.0706 (3)	−0.1097 (4)	0.2805 (3)
C(21)	0.0539 (3)	−0.1722 (5)	0.3101 (3)
C(22)	0.0676 (3)	−0.2494 (5)	0.3012 (3)
C(23)	0.0974 (3)	−0.2653 (4)	0.2637 (3)
C(24)	0.1144 (3)	−0.2029 (4)	0.2342 (3)
C(25)	0.1029 (2)	0.1916 (4)	0.2144 (2)
C(26)	0.0613 (3)	0.2364 (4)	0.2084 (3)
C(27)	0.0594 (2)	0.1832 (3)	0.1218 (3)
C(28)	0.0386 (2)	0.1649 (4)	0.0573 (3)
C(29)	0.2337 (3)	−0.0387 (4)	0.1534 (3)
C(30)	0.2807 (3)	−0.0611 (4)	0.1502 (4)
C(31)	0.2728 (2)	0.0673 (4)	0.1327 (2)
C(32)	0.2874 (3)	0.1482 (4)	0.1168 (3)
O(1)	0.0671 (3)	0.3136 (7)	0.4233 (3)
O(2)	0.0543 (3)	0.3326 (5)	0.3300 (3)
O(3)	0.1356 (3)	0.3161 (5)	0.3882 (5)
O(4)	0.0972 (3)	0.4254 (5)	0.3896 (4)
O(5)	0.4106	0.0273	0.2703
C(33)	0.3925	−0.0379	0.2979
C(34)	0.4259	−0.0458	0.3580
C(35)	0.4636	0.0144	0.3661
C(36)	0.4541	0.0604	0.3111
O(6)	0.4118 (10)	0.0542 (14)	0.1552 (10)

Table II. Selected Bond Lengths in $[Fe(TPP)(2\text{-MeHIm})_2]ClO_4 \cdot THF \cdot H_2O$[a]

type	length, Å	type	length, Å
Fe–N(1)	1.976 (4)	C(a6)–C(m3)	1.397 (7)
Fe–N(2)	1.966 (4)	C(a7)–C(m3)	1.383 (7)
Fe–N(3)	1.968 (4)	C(a8)–C(m4)	1.386 (7)
Fe–N(4)	1.972 (4)	C(b1)–C(b2)	1.356 (7)
Fe–N(5)	2.015 (4)	C(b3)–C(b4)	1.358 (7)
Fe–N(6)	2.010 (4)	C(b5)–C(b6)	1.336 (7)
N(1)–C(a1)	1.383 (6)	C(b7)–C(b8)	1.350 (7)
N(1)–C(a2)	1.392 (6)	C(m1)–C(1)	1.512 (7)
N(2)–C(a3)	1.383 (6)	C(m2)–C(7)	1.495 (7)
N(2)–C(a4)	1.379 (6)	C(m3)–C(13)	1.502 (7)
N(3)–C(a5)	1.372 (6)	C(m4)–C(19)	1.492 (7)
N(3)–C(a6)	1.391 (6)	N(5)–C(25)	1.413 (6)
N(4)–C(a7)	1.380 (6)	N(5)–C(27)	1.331 (6)
N(4)–C(a8)	1.391 (6)	C(25)–C(26)	1.330 (8)
C(a1)–C(b1)	1.446 (7)	C(26)–N(7)	1.374 (7)
C(a2)–C(b2)	1.450 (7)	N(7)–C(27)	1.349 (7)
C(a3)–C(b3)	1.435 (7)	C(27)–C(28)	1.500 (8)
C(a4)–C(b4)	1.440 (7)	N(6)–C(29)	1.396 (7)
C(a5)–C(b5)	1.435 (7)	N(6)–C(31)	1.341 (7)
C(a6)–C(b6)	1.428 (7)	C(29)–C(30)	1.342 (9)
C(a7)–C(b7)	1.434 (7)	C(30)–N(8)	1.358 (8)
C(a8)–C(b8)	1.429 (7)	N(8)–C(31)	1.352 (7)
C(a1)–C(m4)	1.379 (7)	C(31)–C(32)	1.497 (8)
C(a2)–C(m1)	1.381 (7)	Cl–O(1)	1.359 (7)
C(a3)–C(m1)	1.398 (7)	Cl–O(2)	1.363 (6)
C(a4)–C(m2)	1.376 (7)	Cl–O(3)	1.332 (7)
C(a5)–C(m2)	1.400 (7)	Cl–O(4)	1.357 (7)

[a] The estimated standard deviations of the least significant digits are given in parentheses.

Averaged values of porphinato core bond parameters are normal with N–C(a) = 1.384 (7) Å, C(a)–C(b) = 1.437 (8) Å, C(a)–C(m) = 1.388 (9) Å, C(b)–C(b) = 1.350 (7) Å. Averaged values of bond angles are Fe–N–C(a) = 127.0 (7)°, C(a)–N–C(a) = 105.9 (4)°, N–C(a)–C(b) = 109.7 (3)°, N–C(a)–C(m) = 125.4 (4)°, C(a)–C(b)–C(b) = 107.4 (4)°, C(a)–C(m)–C(a) = 123.3 (3)°, and C(a)–C(b)–C(m) = 124.6 (5)°. The numbers in parentheses following each averaged value are the estimated standard deviations calculated on the assumption that the averaged values are all drawn from the same population.

As described in more detail below, the environments of the two axial ligands in $[Fe(TPP)(2\text{-MeHIm})_2]ClO_4$ are essentially identical. The two independent axial Fe–N(2-MeHIm) bond distances of 2.015 (4) and 2.010 (4) Å are equal within experimental error. These axial distances are distinctly longer than those observed with sterically unhindered imidazoles: 1.957 (4) and 1.991 (4) Å in $[Fe(TPP)(HIm)_2]Cl \cdot CH_3OH$,[20a] 1.966 (5) and 1.988 (5) Å in $[Fe(Proto\ IX)(1\text{-MeIm})_2] \cdot CH_3OH \cdot H_2O$,[20b] and 1.964 (3) and 1.977 (3) Å in $[Fe(TPP)(HIm)_2]Cl \cdot CHCl_3 \cdot H_2O$.[20d] In all of these other derivatives the longer axial bond distance is associated with a less favorable orientation for one of the axial imidazoles. Consideration of that orientation effect on the above bond distances along with the observed orientations of the imidazoles in $[Fe(TPP)(2\text{-MeHIm})_2]ClO_4$ lead us to conclude that the axial bonds are "stretched" by no more than 0.03–0.05 Å as a consequence of the effects of the bulky 2-methyl substituents.

The coordination of the two sterically bulky 2-methylimidazole axial ligands and the formation of the low-spin species with nearly normal Fe–N bond distances are the consequence of a variety of structural accommodations. Many, but not all, of these effects have been observed previously. The axial Fe–N bonds are tipped ~4° from the heme normal in such a way as to increase the separation of the methyl substituents from the phorphinato core. Pairs of Fe–N(Im)–C(Im) angles (for each imidazole ring) differ by about 12°, again in a manner that contributes significantly to increasing the methyl···core separations. Finally the two N–C–C(methyl) angles in each ring differ by about 7°, reflecting a bending of the methyl group that again serves to decrease nonbonded interactions. These features can be seen in all other metalloporphyrin complexes with bulky imidazole ligands, including the five-coordinate species where steric problems appear

(23) Scheidt, W. R.; Lee, Y. J. *Struct. Bonding (Berlin)*, in press.

Table III. Selected Bond Angles in [Fe(TPP)(2-MeHIm)$_2$]ClO$_4$·THF·H$_2$O

angle	value, deg	angle	value, deg
N(1)FeN(2)	90.8 (2)	C(a1)C(b1)C(b2)	107.7 (5)
N(2)FeN(3)	89.4 (2)	C(a2)C(b2)C(b1)	107.1 (5)
N(3)FeN(4)	90.4 (2)	C(a3)C(b3)C(b4)	107.5 (5)
N(4)FeN(1)	89.4 (2)	C(a4)C(b4)C(b3)	106.7 (5)
N(5)FeN(1)	89.4 (2)	C(a5)C(b5)C(b6)	107.7 (5)
N(5)FeN(2)	85.3 (2)	C(a6)C(b6)C(b5)	107.4 (5)
N(5)FeN(3)	92.3 (2)	C(a7)C(b7)C(b8)	106.9 (5)
N(5)FeN(4)	93.3 (2)	C(a8)C(b8)C(7)	108.0 (5)
N(6)FeN(1)	87.3 (2)	C(m4)C(a1)C(b1)	124.7 (5)
N(6)FeN(2)	92.6 (2)	C(m1)C(a2)C(b2)	124.2 (5)
N(6)FeN(3)	91.0 (2)	C(m1)C(a3)C(b3)	124.7 (5)
N(6)FeN(7)	88.8 (2)	C(m2)C(a4)C(b4)	124.1 (5)
N(1)FeN(3)	178.3 (8)	C(m2)C(a5)C(b5)	125.4 (5)
N(2)FeN(4)	178.6 (5)	C(m3)C(a6)C(b6)	125.0 (5)
N(5)FeN(6)	176.1 (5)	C(m3)C(a7)C(b7)	124.1 (5)
FeN(1)C(a1)	127.8 (3)	C(m4)C(a8)C(b8)	125.0 (5)
FeN(1)C(a2)	125.5 (3)	C(a2)C(m1)C(a3)	123.4 (5)
FeN(2)C(a3)	127.1 (3)	C(a4)C(m2)C(a5)	123.1 (5)
FeN(2)C(a4)	126.7 (3)	C(a6)C(m3)C(a7)	123.7 (5)
FeN(3)C(a5)	127.7 (3)	C(a8)C(m4)C(a1)	123.0 (5)
FeN(3)C(a6)	126.8 (4)	C(a2)C(m1)C(1)	118.0 (5)
FeN(4)C(a7)	126.8 (3)	C(a3)C(m1)C(1)	118.3 (5)
FeN(4)C(a8)	127.5 (3)	C(a4)C(m2)C(7)	118.4 (5)
FeN(5)C(25)	120.6 (4)	C(a5)C(m2)C(7)	118.3 (5)
FeN(5)C(27)	133.2 (4)	C(a6)C(m3)C(13)	118.7 (5)
FeN(6)C(29)	120.5 (4)	C(a7)C(m3)C(13)	117.4 (5)
FeN(6)C(31)	132.5 (4)	C(a8)C(m4)C(19)	119.3 (5)
C(a1)N(1)C(a2)	106.5 (4)	C(a1)C(m4)C(19)	117.4 (5)
C(a3)N(2)C(a4)	105.8 (4)	C(25)N(5)C(27)	105.6 (5)
C(a5)N(3)C(a6)	105.5 (4)	N(5)C(25)C(26)	109.0 (5)
C(a7)N(4)C(a8)	105.7 (4)	C(25)C(26)N(7)	107.2 (5)
N(1)C(a1)C(b1)	109.4 (5)	C(26)N(7)C(27)	108.0 (5)
N(1)C(a2)C(b2)	109.3 (5)	N(7)C(27)N(5)	110.1 (5)
N(2)C(a3)C(b3)	109.8 (5)	N(7)C(27)C(28)	120.9 (5)
N(2)C(a4)C(b4)	110.2 (4)	N(5)C(27)C(28)	129.0 (6)
N(3)C(a5)C(b5)	109.8 (5)	C(27)N(6)C(31)	106.7 (5)
N(3)C(a6)C(b6)	109.7 (5)	N(6)C(29)C(30)	108.7 (6)
N(4)C(a7)C(b7)	110.0 (5)	C(29)C(30)N(8)	106.8 (6)
N(4)C(a8)C(b8)	109.3 (4)	C(30)N(8)C(31)	109.5 (5)
N(1)C(a1)C(m4)	125.7 (5)	N(8)C(31)N(6)	108.3 (6)
N(1)C(a2)C(m1)	125.9 (5)	N(8)C(31)C(32)	122.5 (6)
N(2)C(a3)C(m1)	125.2 (5)	N(6)C(31)C(32)	129.1 (6)
N(2)C(a4)C(m2)	125.5 (5)	O(1)ClO(2)	103.9 (4)
N(3)C(a5)C(m2)	124.8 (5)	O(1)ClO(3)	109.8 (6)
N(3)C(a6)C(m3)	124.8 (5)	O(1)ClO(4)	114.0 (6)
N(4)C(a7)C(m3)	125.8 (5)	O(2)ClO(3)	115.6 (6)
N(4)C(a8)C(m4)	125.3 (5)	O(2)ClO(4)	109.3 (6)
		O(3)ClO(4)	104.4 (5)

to be much less severe. The magnitudes of the three effects are similar in low-spin [Co(TPP)(1,2-DiMeIm)],[24] high-spin ferrous [Fe(TpivPP)(2-MeHIm)] and low-spin [Fe(TpivPP)(2-MeHIm)(O$_2$)],[25] high-spin five-coordinate [Fe(OEP)(2-MeHIm)]$^+$,[6] and high-spin six-coordinate [Fe(OEP)(2-MeHIm)$_2$]$^+$.[11] With regard to the closest approach of imidazole atoms to the core, it should be noted that these effects lead to closer contacts of the α-hydrogen atom than of the methyl-hdyrogen atoms. (In all cases where hydrogen atoms have been experimentally located the methyl group hydrogen atoms are found to have one hydrogen atom away from the core with the C–H vector nearly coplanar with the imidazole plane.)

The projection of the imidazole planes onto the porphinato core makes angles ϕ of $\sim$32° with the respective closest Fe–N$_p$ bond. The usual values of this angle are much closer to zero or, in other words, close to eclipsing a coordinating M–N$_p$ bond. Scheidt and Chipman[26] have given a theoretical explanation of the tendency toward small values for ϕ in imidazole complexes. The observed

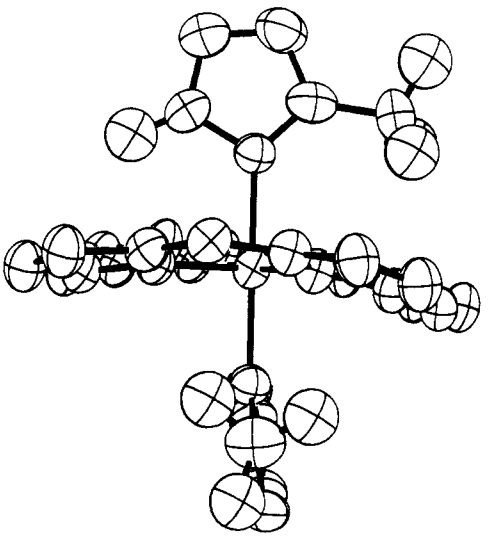

Figure 4. Diagram illustrating the fitting of the methyl groups into the S_4-ruffled core. For clarity, the phenyl groups are not displayed and only the methyl and α-carbon atom hydrogens of the imidazole rings are shown.

rotations of the imidazoles about the heme normal also help to alleviate the steric interactions of the methyl groups as described below. The most significant features that allow both coordination of the two 2-methylimidazoles and formation of a low-spin complex are the S_4 ruffling of the porphinato core and the mutually perpendicular arrangement of the two axial ligands. These two structural features, in combination with the ϕ angles of 32°, allow each 2-methyl group to fit into the hollows formed by alternating displacements of the methine carbon atoms from the mean plane of the 24-atom core. The nearly mutually perpendicular[27] alignment of the two imidazole planes is thus seen to arise from a need to accommodate the bulky methyl groups. These stereochemical features are clearly seen in Figure 4. Figure 4 also illustrates two other effects which aid in accommodating the bulky methyl groups: a tilting of the imidazole plane from the normal to the porphinato core and an apparent rotation of the methyl group hydrogen atoms. Figure 4 makes it evident that the directions of both effects serve to minimize H···core atom nonbonded contacts. The tilt of the two imidazole rings (the dihedral angle between the core and the imidazole ring) is 79.4° for ring N(5) and 85.7° for ring N(6). The precise location of the hydrogen atoms is known with less certainty because only five of the six hydrogen atom positions were located experimentally.

The N–H protons of both imidazoles form hydrogen bonds: H(N7) to a perchlorate oxygen and H(N8) to the water molecule. Observed heavy-atom distances are N(7)···O(2) = 3.06 Å and N(8)···O(6) = 2.93 Å.

It is to be noted that the perpendicular orientation of the two bulky ligands, coupled with the S_4 ruffling of the core, appears to be the only feasible stereochemical way in which a low-spin geometry could be achieved. A second stereochemical solution for the coordination of two bulky 2-methylimidazole ligands is to form a species with longer axial bonds; such species could be either[28] a high-spin or an intermediate-spin complex. The high-spin complex [Fe(OEP)(2-MeHIm)$_2$]ClO$_4$[11] has been isolated and the structure has been determined. Surprisingly, the two different species appear equally efficacious in "solving" the steric problems as judged by nonbonded separations—especially those involving the imidazole hydrogen atoms. This can be seen in Table IV where stereochemical parameters of the axial ligands of [Fe(TPP)(2-MeHIm)$_2$]ClO$_4$ and [Fe(OEP)(2-MeHIm)$_2$]ClO$_4$ are noted. The positions of hydrogen atoms in Table IV have been corrected to equilibrium C–H distances of 1.08 Å rather than the X-ray

(24) Dwyer, P. N.; Madura, P.; Scheidt, W. R. *J. Am. Chem. Soc.* **1974**, *96*, 4815–4819.
(25) Jameson, G. B.; Molinaro, F. S.; Ibers, J. A.; Collman, J. P.; Brauman, J. I.; Rose, E.; Suslick, K. S. *J. Am. Chem. Soc.* **1980**, *102*, 3224–3237.
(26) Scheidt, W. R.; Chipman, D. M. *J. Am. Chem. Soc.* **1986**, *108*, 1163–1167.
(27) The dihedral angle between the two axial ligand planes is 89.3°.
(28) Scheidt, W. R.; Gouterman, M. In *Iron Porphyrins*, Part I; Lever, A. B. P., Gray, H. B., Eds.; Addison-Wesley: Reading MA, 1983; pp 89–139.

Table IV. Comparison of Axial Ligand Parameters in Low-Spin $[Fe(TPP)(2\text{-}MeHIm)_2]ClO_4 \cdot THF \cdot H_2O$ and High-Spin $[Fe(OEP)(2\text{-}MeHIm)_2]ClO_4$[a]

	$[Fe(TPP)(2\text{-}MeHIm)_2]^+$		
	ring 1	ring 2	$[Fe(OEP)(2\text{-}MeHIm)_2]^+$[b]
$Fe\text{-}N_{ax}$ (Å)	2.015 (4)	2.010 (4)	2.227 (2)
$Fe\text{-}N_{ax}$ tip (deg)	5.6	3.6	3.2
Δ(Fe–N–C) (deg)	12.6	12.0	13.4
$\Delta(N\text{-}C\text{-}C_{methyl})$ (deg)	8.1	6.6	6.5
ϕ (deg)	32.7	32.3	22.2
dihedral angles Im to core (deg)	79.4	85.8	86.1
α-C–H contacts (Å)	H(25)···N1 2.58	H(29)···N4 2.54	H(3)···Ca3 2.55
	H(25)···Ca2 2.65	H(29)···Ca8 2.60	H(3)···N2 2.59
	H(25)···Cm1 2.80	H(29)···Cm4 2.80	H(3)···Cm2 2.83
Me H contacts (Å)	H(28a)···Ca7 2.67	H(32a)···N2 2.62	H(4a)···Ca3 2.45
	H(28a)···Cm3 2.76	H(32a)···Ca4 2.79	H(4a)···Cm2 2.55
	H(28a)···N4 2.77	H(32a)···Ca3 2.82	H(4a)···N2 2.79
	H(28b)···N3 2.59	H(32b)···Ca5 2.61	H(4b)···N2 3.03
	H(28b)···Ca5 2.64	H(32b)···Cm2 2.73	H(4b)···Ca4 3.04
	H(28b)···Ca6 2.74	H(32b)···N3 2.80	H(4b)···Ca3 3.12

[a] All atomic labeling uses original notation. [b] Complex has a crystallographic inversion center.

distances. The near equivalence of nonbonded distances between the two species in Table IV makes it clear that a 10° change in imidazole orientation, coupled with a S_4 ruffling of the core, is approximately equivalent to an increase of 0.26 Å in the axial bond length.

Despite the apparent equivalence of the two molecular structures, it is not clear just what leads to one spin state over another for *isolated, solid-state* species containing sterically hindered ligands. In our hands,[29] attempts to prepare additional low-spin complexes with hindered imidazoles lead to the isolation of either high-spin bis(hindered imidazole) complexes or the starting ferric porphyrinate. Two such high-spin complexes have been characterized, $[Fe(OEP)(2\text{-}MeHIm)_2]ClO_4$[11] and $[Fe(TPP)(BzHIm)_2]ClO_4$.[30] However, low-temperature (frozen solution, 20 K) EPR spectra[31] do show the formation of low-spin species under the preparative conditions, which suggests that the low-spin state is the ground state in solution. As noted above, there are two specific ligand orientation requirements that we believe are needed to form hindered ligand low-spin species: relatively large values of ϕ and a mutually perpendicular alignment of the two axial planes. Theoretical calculations[26] suggest that small values of ϕ are favored owing to an imidazole $p\pi$ to metal $4p\pi$ interaction. Further, for low-spin ferric species, parallel ligand orientations are favored to maximize imidazole $p\pi$ to metal $3d\pi$ overlaps. Thus both observed ligand orientation effects would appear to reduce the stability of the present low-spin species relative to a low-spin species with normal unhindered axial imidazoles. Presumably, these unfavorable orientation effects lead to a small energy difference between the low-spin and high-spin states. Interestingly, Mössbauer spectra[31] of $[Fe(TPP)(2\text{-}MeHIm)_2]ClO_4$ in both the bulk solid and solution state show the presence of a small amount of a high-spin species, but we see no evidence for a high-spin species in the X-ray structure.

Finally, a recent survey[23] of relative orientations of bis(imidazole) complexes shows that nearly all have precisely or nearly parallel relative imidazole plane orientations. It has been suggested[31] that the kind of unusual perpendicular arrangement of the two axial ligands seen in the present complex is related to a novel low-spin EPR spectrum, the so-called strong g_{max} signal. Low-spin ferric derivatives that display this strong g_{max} signal have a $g > 3.3$ as the only observable spectral feature and the signal is observed only at temperatures below about 30 K. $[Fe(TPP)(2\text{-}MeHIm)_2]ClO_4$ now becomes the only imidazole-ligated ferric porphyrinate of *known* structure that displays[32] this strong g_{max} signal. As noted above, the mutually perpendicular alignment is required to allow formation of a low-spin complex. This alignment leads to near axial symmetry, effective degeneracy of the d_{xz} and d_{yz} orbitals, and hence the large g-value signal. These features may be quite general, and the relevance to biological systems and the possible implications for control of redox potential have been discussed.[31] The apparent requirement of near axial symmetry is further confirmed by the finding of Strouse[33] that $K[Fe(TPP)(CN)_2]$[21b] also displays a strong g_{max} signal. In this latter complex, the electronic axial symmetry results directly from the axially symmetric ligands rather than a ligand orientation effect.

Acknowledgment. We thank the National Institutes of Health (Grant HL-15627 to W.R.S., Grant GM-09370 to J.L.H.) and the National Science Foundation (Grant CHE-8519913 to C. A.R.) for support of this work.

Supplementary Material Available: Table IS, listing of calculated hydrogen atom positions, Table IIS, anisotropic thermal parameters, Table IIIS, magnetic susceptiblity data, and Figure 1S, a plot of $1/\chi_m$ vs. T and μ_B vs. T for the chloroform solvate (9 pages); listings of observed and calculated structure amplitudes (×10) (31 pages). Ordering information is given on any current masthead page.

(29) Osvath, S. R.; Scheidt, W. R., unpublished results. We have been able to produce one additional low-spin complex, $[Fe(Tp\text{-}OCH_3PP)(BenzHIm)_2]ClO_4$, but have not obtained crystals large enough for a structure determination.

(30) Levan, K. R.; Strouse, C. E. *Abstract of Papers*; American Crystallolgraphic Association Summer Meeting, Snowmass, CO, Aug 1–5, 1983; Abstract H1. Levan, K. R. Ph.D. Thesis, UCLA, 1984.

(31) Walker, F. A.; Huynh, B. H.; Scheidt, W. R.; Osvath, S. R. *J. Am. Chem. Soc.* **1986**, *108*, 5288–5297.

(32) The strong g_{max} signal is given by a number of hindered imidazole and low-basicity pyridines in frozen solution. However, all other low-spin bis(imidazole) species of known structure give normal "class B" EPR signals. See ref 31 and the following: Walker, F. A.; Reis, D.; Balke, V. L. *J. Am. Chem. Soc.* **1984**, *106*, 6888–6898 and references cited therein.

(33) St. John, E. G.; Strouse, C. E., personal communication.